Stability analysis and design of amplitude death induced by a time-varying delay connection

Stability analysis and design of amplitude death induced by a time-varying delay connection

Keiji Konishi Hideki Kokame Naoyuki Hara

Department of Electrical and Information Systems, Osaka Prefecture University
1–1 Gakuen-cho, Naka-ku, Sakai, Osaka 599-8531, Japan

Abstract

The present paper considers amplitude death in a pair of oscillators coupled by a time-varying delay connection. A linear stability analysis is used to derive the boundary curves for amplitude death in a connection parameters space. The delay time can be arbitrarily long for certain amplitude of delay variation and coupling strength. A simple systematic procedure for designing such variation and strength is provided. The theoretical results are verified by a numerical simulation.

Key words: amplitude death, delayed feedback control, time-varying delay
PACS: 05.45.Xt, 05.45.Gg, 05.45.-a

---

1 Introduction

Nonlinear phenomena in coupled oscillators have received considerable attention not only from academia [1], but also from the engineering community [2]. Amplitude death, one such nonlinear phenomenon, has been the subject of numerous research papers [3,4]. Amplitude death can be considered to be the stabilization of an unstable steady state of oscillators induced by diffusive connections. Amplitude death was reported never to occur in identical coupled oscillators [4,5]. However, in 1998, Reddy *et al.* showed that a transmission delay in connections can induce amplitude death even when the oscillators are identical [6]. This phenomenon, referred to as time-delay induced amplitude death, has attracted growing interest in the field of nonlinear physics [7]. This phenomenon has been investigated extensively in recent years [8–21].

Since amplitude death is the stabilization of unstable behavior in coupled nonlinear systems, this phenomenon has significant potential for practical application. In laser systems, the delayed connections can be implemented by optical mutual coupling [22]. However, for the case in which the laser systems must be placed at a great distance due to practical consideration, the delay time in the connections must be long. However, long delay times tend to destabilize dynamical systems. Thus, for the above case, a short delay time in connections cannot be implemented experimentally, and so the stabilization of unstable systems becomes difficult. For researchers who want to induce amplitude death, it is important to overcome this difficulty. Atay showed that distributed delay connections facilitate amplitude death [14]: the long distributed delay times can induce amplitude death. Konishi *et al.* reported that the multiple long delay connections can also induce amplitude death in a pair of oscillators [23,24]. Although these studies have presented useful solutions, they also suffer from some disadvantages. For example, the distributed delay connections would be difficult to implement in industrial systems, such as laser systems and electronic oscillators; the implementation cost of the multiple delay connections would be higher than that of the single delay connection, since the multiple delay-devices are required for the implementation.

These studies on amplitude death dealt with coupled oscillators. In recent years, the significant results on stability of a single system with time-varying delay have been reported in the field of control theory: Michiels, Assche, and Niculescu showed that the stability of a time-varying point-wise delay system is equivalent to that of a time-invariant distributed delay system [25] and demonstrated through three numerical examples that the time-varying point-wise delay leads to larger stability regions; Gjurchinovski and Urumov applied the stability analysis of the time-varying delay systems to delayed feedback control systems [26].

The present paper considers a pair of oscillators coupled by a time-varying delay connection. The stability analysis based on the analytical results [25] shows that such connection can induce amplitude death in the coupled oscillators. We emphasize that the time-varying delay connection overcomes the disadvantages reported in previous studies [14,23,24]. Therefore, there is no need to implement the distributed delay or multiple delay-devices. In the present study, we analyze the stability of amplitude death and provide a systematic procedure to design connections such that the nominal delay time is arbitrary long. A numerical simulation is conducted to verify the theoretical results.
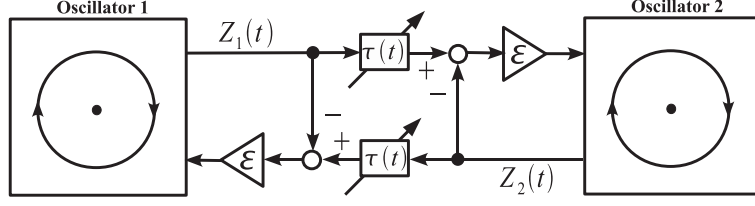
2

Fig. 1. Block diagram of a pair of oscillators (1) coupled by connections (2).

2 Coupled limit cycle oscillators

Consider a pair of oscillators (see Fig. 1)[1],

$$\dot{Z}_{1,2}(t) = \left\{ \mu + i\omega - |Z_{1,2}(t)|^2 \right\} Z_{1,2}(t) + u_{1,2}(t), \tag{1}$$

where $Z_{1,2}(t) \in \mathbb{C}$ are the state variables, and $\mu > 0$ and $\omega > 0$ represent the degree of instability of the fixed points $Z_{1,2}^* = 0$ and the oscillator frequency, respectively. Here, i is defined as $i = \sqrt{-1}$. The coupling signals $u_{1,2}(t) \in \mathbb{C}$ are given by

$$u_{1,2}(t) = \varepsilon \left\{ Z_{2,1}(t - \tau(t)) - Z_{1,2}(t) \right\}, \tag{2}$$

where $\varepsilon > 0$ is the coupling strength. The time delay $\tau(t) \geq 0$ in coupling signals varies around a nominal delay $\tau_0 > 0$ with amplitude $\delta \in [0, \tau_0]$,

$$\tau(t) := \tau_0 + \delta f(\Omega t). \tag{3}$$

$\Omega > 0$ is the frequency of variation. In the present study, we consider the periodic sawtooth type function,

$$f(x) := \begin{cases} +\dfrac{2}{\pi} \left(x - \dfrac{\pi}{2} - 2n\pi \right) & \text{if } x \in [2n\pi, (2n+1)\pi), \\[2mm] -\dfrac{2}{\pi} \left(x - \dfrac{3\pi}{2} - 2n\pi \right) & \text{if } x \in [(2n+1)\pi, 2(n+1)\pi), \end{cases} \tag{4}$$

for $n = 0, 1, \ldots$, since this type delay can be actualized easily in experimental situations and be simply analyzed. Oscillators (1) with connections (2) have the homogeneous steady state: $\boldsymbol{Z}^* := [Z_1^* \ Z_2^*]^T = [0 \ 0]^T$. Here, $Z_{1,2}(t) = Z^* + z_{1,2}(t)$, where $z_{1,2}(t) \in \mathbb{C}$ are the variations of the oscillator around $Z_{1,2}^*$, are substituted into the coupled oscillator. The linearization of the coupled oscillator at $\boldsymbol{Z}^* = 0$ allows us to obtain

$$\dot{z}_{1,2}(t) = (\mu + i\omega) z_{1,2}(t) + \varepsilon \left\{ z_{2,1}(t - \tau(t)) - z_{1,2}(t) \right\}. \tag{5}$$

---

[1] Remark that, since each oscillator is the normal form for the Hopf bifurcation [27], the analytical results in the present paper are valid for the oscillators where oscillations occur through such a bifurcation.

3

Linearized system (5) can be rewritten as

$$\dot{\boldsymbol{x}}(t) = \boldsymbol{A}\boldsymbol{x}(t) + \boldsymbol{B}\boldsymbol{x}(t - \tau(t)), \tag{6}$$

where

$$\boldsymbol{x}(t) := \begin{bmatrix} \mathrm{Re}(z_1(t)) \\ \mathrm{Im}(z_1(t)) \\ \mathrm{Re}(z_2(t)) \\ \mathrm{Im}(z_2(t)) \end{bmatrix}, \quad \boldsymbol{A} := \begin{bmatrix} \mu - \varepsilon & -\omega & 0 & 0 \\ \omega & \mu - \varepsilon & 0 & 0 \\ 0 & 0 & \mu - \varepsilon & -\omega \\ 0 & 0 & \omega & \mu - \varepsilon \end{bmatrix}, \quad \boldsymbol{B} := \begin{bmatrix} 0 & 0 & \varepsilon & 0 \\ 0 & 0 & 0 & \varepsilon \\ \varepsilon & 0 & 0 & 0 \\ 0 & \varepsilon & 0 & 0 \end{bmatrix}.$$

According to Ref. [25], if a time-invariant comparison system,

$$\dot{\boldsymbol{x}}(t) = \boldsymbol{A}\boldsymbol{x}(t) + \frac{1}{2\delta}\boldsymbol{B}\int_{t-\tau_0-\delta}^{t-\tau_0+\delta} \boldsymbol{x}(\theta)\mathrm{d}\theta, \tag{7}$$

is asymptotically stable, then linear system (6), including delay time (3) with sawtooth function (4), is stable for large Ω. The stability of system (7) is governed by the roots of its characteristic equation,

$$g(\lambda) := \det\left[\lambda\boldsymbol{I} - \boldsymbol{A} - \boldsymbol{B}e^{-\lambda\tau_0}h(\lambda\delta)\right] = 0, \tag{8}$$

where

$$h(\lambda\delta) := \begin{cases} (\sinh\lambda\delta)/(\lambda\delta) & \text{if } \lambda\delta \neq 0, \\ 1 & \text{if } \lambda\delta = 0. \end{cases}$$

Equation (8) is derived by substituting $\boldsymbol{x}(t) = \boldsymbol{b}e^{\lambda t}$ into Eq. (7). The characteristic function $g(\lambda)$ in Eq. (8) can be described by $g(\lambda) := g_1(\lambda)g_2(\lambda)$, where

$$\begin{aligned} g_1(\lambda) &:= \left\{\lambda - \mu + \varepsilon\left(1 - e^{-\lambda\tau_0}h(\lambda\delta)\right)\right\}^2 + \omega^2, \\ g_2(\lambda) &:= \left\{\lambda - \mu + \varepsilon\left(1 + e^{-\lambda\tau_0}h(\lambda\delta)\right)\right\}^2 + \omega^2. \end{aligned} \tag{9}$$

The homogeneous steady state $\boldsymbol{Z}^*$ is stable if and only if all of the roots λ for the equations $g_1(\lambda) = 0$ and $g_2(\lambda) = 0$ lie in the open left-half complex plane.

3 Stability analysis

In this section, we investigate the characteristic equations $g_1(\lambda) = 0$ and $g_2(\lambda) = 0$. First, we focus on the stability of $g_1(\lambda) = 0$. Substituting $\lambda = i\lambda_I$ into $g_1(\lambda) = 0$, its real and imaginary parts are estimated:

$$\varepsilon - \mu - \varepsilon\Phi(\lambda_I)\cos\lambda_I\tau_0 = 0, \quad \lambda_I - \omega + \varepsilon\Phi(\lambda_I)\sin\lambda_I\tau_0 = 0, \tag{10}$$

4

where

$$\Phi(\lambda_I) := \begin{cases} (\sin \lambda_I \delta)/(\lambda_I \delta) & \text{if } \lambda_I \delta \neq 0, \\ 1 & \text{if } \lambda_I \delta = 0. \end{cases}$$

From Eq. (10), we obtain the relation between ε and λ_I,

$$F(\varepsilon, \lambda_I) := \left\{ 1 - \Phi(\lambda_I)^2 \right\} \varepsilon^2 - 2\mu\varepsilon + \mu^2 + (\lambda_I - \omega)^2 = 0, \tag{11}$$

which is independent of τ_0. The solution $\varepsilon(\lambda_I)$ of Eq. (11) with $\lambda_I \neq 0$ is

$$\varepsilon(\lambda_I) = \frac{\mu \pm \sqrt{D(\lambda_I)}}{1 - \Phi(\lambda_I)^2}, \quad D(\lambda_I) := \Phi(\lambda_I)^2 \mu^2 - (1 - \Phi(\lambda_I)^2)(\omega - \lambda_I)^2, \tag{12}$$

where $0 < \Phi(\lambda_I)^2 \leq 1$. As $D(\lambda_I)$ is a discriminant for ε, there exist two positive solutions $\varepsilon(\lambda_I)$ when $D(\lambda_I) > 0$. Since $\lim_{\lambda_I \to 0} D(\lambda_I) = \mu^2 > 0$ and $\lim_{\lambda_I \to +\infty} D(\lambda_I) = -\infty$ ($\lim_{\lambda_I \to -\infty} D(\lambda_I) = -\infty$), there exist $2\overline{m} + 1$ positive ($2\underline{m} + 1$ negative) real roots of $D(\lambda_I) = 0$. Let the real roots $\lambda^*_{I_j}$ have the following relation:

$$\lambda^*_{I_{-(2\underline{m}+1)}} \leq \cdots \leq \lambda^*_{I_{-2}} \leq \lambda^*_{I_{-1}} < 0 < \lambda^*_{I_1} \leq \lambda^*_{I_2} \leq \cdots \leq \lambda^*_{I_{2\overline{m}+1}}.$$

Then, there exist two positive $\varepsilon(\lambda_I)$ for $\lambda_I \in (\Lambda_- \cup \Lambda_0 \cup \Lambda_+)$, where

$$\Lambda_- := \bigcup_{l=1}^{\underline{m}} \left(\lambda^*_{I_{-(2l+1)}}, \lambda^*_{I_{-2l}} \right), \quad \Lambda_0 := \left(\lambda^*_{I_{-1}}, \lambda^*_{I_1} \right), \quad \Lambda_+ := \bigcup_{l=1}^{\overline{m}} \left(\lambda^*_{I_{2l}}, \lambda^*_{I_{2l+1}} \right).$$

The boundary curves are obtained by the following procedure. First, λ_I is varied in the range $\lambda_I \in (\Lambda_- \cup \Lambda_0 \cup \Lambda_+)$. Then, $\varepsilon(\lambda_I)$ in Eq. (12) and $\tau_0(n, \lambda_I)$ of Eq. (10),

$$\tau_0(n, \lambda_I) := \begin{cases} \left\{ \bar{\tau}_0(\lambda_I) + 2n\pi \right\} / \lambda_I & \text{if } (\varepsilon(\lambda_I) - \mu)/\Phi(\lambda_I) > 0, \\ \left\{ \bar{\tau}_0(\lambda_I) + (2n+1)\pi \right\} / \lambda_I & \text{if } (\varepsilon(\lambda_I) - \mu)/\Phi(\lambda_I) < 0, \end{cases} \tag{13}$$

$$\bar{\tau}_0(\lambda_I) := \text{Tan}^{-1} \left(\frac{\omega - \lambda_I}{\varepsilon(\lambda_I) - \mu} \right), \tag{14}$$

for $n = 0, 1, \ldots$, are plotted in the parameter space ε and τ_0. The terminology Tan^{-1} denotes the principal value of the arc tangent. Furthermore, in order to investigate the direction in which the roots cross the imaginary axis, we must check the sign of the real part of $d\lambda/d\varepsilon$ in Eq. (10) by

$$\text{Re}\left[\frac{d\lambda}{d\varepsilon}\right]_{\substack{\lambda = i\lambda_I \\ \varepsilon = \varepsilon(\lambda_I)}} = \text{Re}\left[\frac{e^{i\lambda_I r^{(-)}} - e^{-i\lambda_I r^{(+)}} - i2\lambda_I \delta}{i2\lambda_I \delta - \varepsilon \left\{ (r^{(-)} + i/\lambda_I)e^{i\lambda_I r^{(-)}} + (r^{(+)} - i/\lambda_I)e^{-i\lambda_I r^{(+)}} \right\}}\right],$$
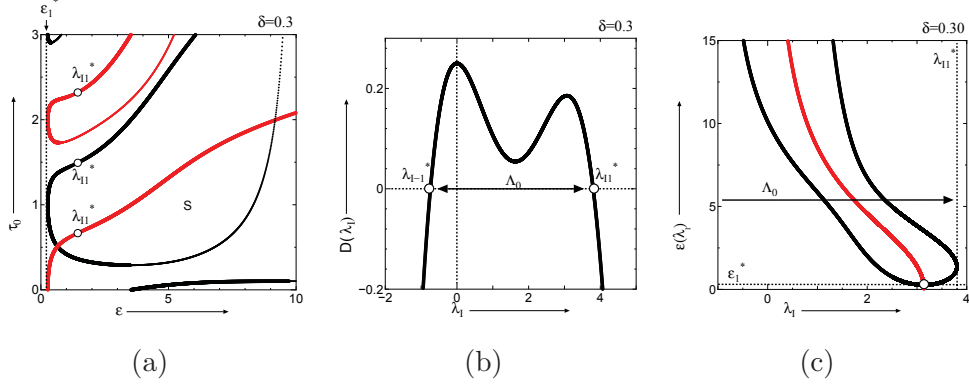
Fig. 2. Boundary curves, discriminant, solutions of $F(\varepsilon, \lambda_I) = 0$ and $G(\varepsilon, \lambda_I) = 0$ for $\delta = 0.30$. (a) Boundary curves in parameter space $\varepsilon - \tau_0$. (b) Discriminant $D(\lambda_I)$. (c) Solutions of $F(\varepsilon, \lambda_I) = 0$ and $G(\varepsilon, \lambda_I) = 0$.

$$(15)$$

where $r^{(\pm)} := \delta \pm \tau_0(n, \lambda_I)$. Then, $\tau_0(n, \lambda_I)$ and λ_I are the values estimated in the above procedure. With increasing ε, a positive (negative) value of Eq. (15) corresponds to a root crossing the axis from left to right (right to left). The above procedure for obtaining the boundary curves is also valid for $g_2(\lambda) = 0$.

Let us next consider numerical examples for the delay amplitude $\delta = 0.30$ and 0.38. The parameters of oscillators are fixed at $\omega = \pi$ and $\mu = 0.5$. It should be noted that although these values are fixed throughout this paper, the analytical results in the present paper are valid for other values. The boundary curves obtained by the above procedure for $\delta = 0.30$ are shown in Fig. 2(a). The black and red curves are the solution of $g_1(i\lambda_I) = 0$ and $g_2(i\lambda_I) = 0$, respectively. A root of $g_{1,2}(i\lambda_I) = 0$ crosses the imaginary axis from left to right (right to left), where the parameters ε and τ_0 are on a thin (bold) curve. The region S bounded by the curves represents the stability region, where there exists no positive root of $g_{1,2}(\lambda) = 0$. The discriminant $D(\lambda_I)$ in Eq. (12) is plotted as shown in Fig. 2(b). The equation $D(\lambda_I) = 0$ has only the two roots $\lambda_{I_{-1}}^*$ and $\lambda_{I_1}^*$, and does not have the ranges Λ_- and Λ_+. The boundary curves with $\varepsilon(\lambda_I)$ and $\tau_0(n, \lambda_I)$ are plotted for $\lambda_I \in \Lambda_0$. The solution of $F(\varepsilon, \lambda_I) = 0$ is plotted using black curves in Fig. 2(c). There exists the bottom of $\varepsilon(\lambda_I)$, which is described by $\varepsilon_1^* = \min_{\lambda_I \in \Lambda_0} \varepsilon(\lambda_I)$. Thus, there is no $\varepsilon(\lambda_I)$ for $\varepsilon < \varepsilon_1^*$. As indicated in Fig. 2(a), region S has an upper limit of $\tau_0 \simeq 2$, which implies that, for $\delta = 0.30$, the coupling signals with the long nominal delay $\tau_0 \gtrsim 2$ cannot induce the stabilization.

The boundary curves for $\delta = 0.38$ are shown in Fig. 3(a). The equation $D(\lambda_I) = 0$ has the four roots $\lambda_{I_j}^*$ ($j = -1, 1, 2, 3$), as shown in Fig. 3(b). Then, we have $\Lambda_- = \emptyset$, $\Lambda_0 = \left(\lambda_{I_{-1}}^*, \lambda_{I_1}^*\right)$, and $\Lambda_+ = \left(\lambda_{I_2}^*, \lambda_{I_3}^*\right)$. There ex-
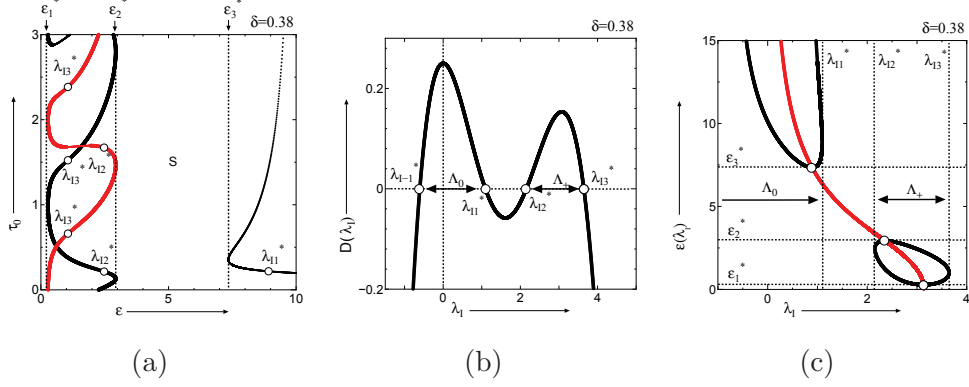
6

Fig. 3. Boundary curves, discriminant, solutions of $F(\varepsilon, \lambda_I) = 0$ and $G(\varepsilon, \lambda_I) = 0$ for $\delta = 0.38$. (a) Boundary curves in parameter space $\varepsilon - \tau_0$. (b) Discriminant $D(\lambda_I)$. (c) Solutions of $F(\varepsilon, \lambda_I) = 0$ and $G(\varepsilon, \lambda_I) = 0$.
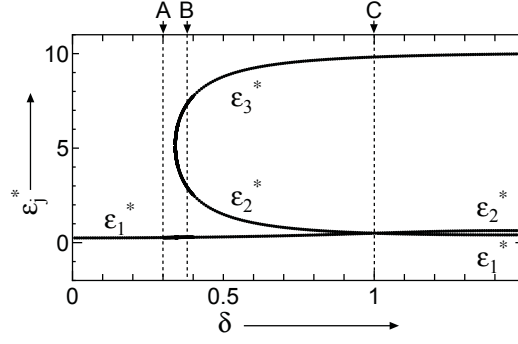

Fig. 4. Relationship between the extreme values ε_j^* and the time-varying delay amplitude δ.

ist the boundary curves for $\lambda_I \in (\Lambda_0 \cup \Lambda_+)$. The solutions of $F(\varepsilon, \lambda_I) = 0$ are shown in Fig. 3(c), where the three extreme values $\varepsilon_1^* = \min_{\lambda_I \in \Lambda_+} \varepsilon(\lambda_I)$, $\varepsilon_2^* = \max_{\lambda_I \in \Lambda_+} \varepsilon(\lambda_I)$, and $\varepsilon_3^* = \min_{\lambda_I \in \Lambda_0} \varepsilon(\lambda_I)$ are the bottom or top of the black curves.

The extreme values ε_j^* ($j = 1, \ldots, q$), which satisfy $\{ d\varepsilon(\lambda_I)/d\lambda_I \}_{\varepsilon = \varepsilon_j^*} = 0$, where q is the number of extreme values, is examined. These values are arranged in ascending order, $0 < \varepsilon_1^* \leq \cdots \leq \varepsilon_q^*$. The equation $F(\varepsilon, \lambda_I) = 0$ is differentiated with λ_I. Substituting $d\varepsilon(\lambda_I)/d\lambda_I = 0$ into the differentiated equation, we obtain

$$G(\varepsilon, \lambda_I) := \varepsilon^2 \Phi(\lambda_I) \{ \cos \lambda_I \delta - \Phi(\lambda_I) \} - \lambda_I (\lambda_I - \omega) = 0. \tag{16}$$

As shown in Figs. 2(c) and 3(c), the black curves $F(\varepsilon, \lambda_I) = 0$ intersect with the red curve $G(\varepsilon, \lambda_I) = 0$ at ε_j^* ($j = 1, \ldots, q$). These values ε_j^* can be estimated by solving the equations $F(\varepsilon, \lambda_I) = 0$ and $G(\varepsilon, \lambda_I) = 0$ numerically. A plot of the values ε_j^* with respect to δ is shown in Fig. 4. For $\delta < 0.341$, there exists the only one extreme value ε_1^*. The boundary curves at point A (i.e.,

7

$\delta = 0.30$) in Fig. 4 are shown in Fig. 2(a). The two extreme values, ε_2^* and ε_3^*, appear at $\delta = 0.341$. For $\delta > 0.341$, there exist the three extreme values $\varepsilon_1^* \leq \varepsilon_2^* < \varepsilon_3^*$. The boundary curves at point B (i.e., $\delta = 0.380$) in Fig. 4 are shown in Fig. 3(a).

Note that there exists no curve in the range $\varepsilon \in (\varepsilon_2^*, \varepsilon_3^*)$ on the parameter space ε and τ_0 for $\delta = 0.38$. In other words, the region S seems to have no upper limit of τ_0. Therefore, if ε is set to $\varepsilon \in (\varepsilon_2^*, \varepsilon_3^*)$, then the steady state $\boldsymbol{Z}^*$ is stabilized by the arbitrarily-long nominal delay τ_0.

4 Design of connection parameters

From the numerical analysis mentioned in the preceding section, we can determine the connection parameters ε and δ such that $\boldsymbol{Z}^*$ is stabilized for any long nominal delay τ_0. However, this analysis is time-consuming, particularly for researchers who merely want to know the parameters.

We focus on the situation in which ε_1^* and ε_2^* are the same at $\delta = \pi/\omega$ (see point C, $\delta = \pi/\omega = 1$, in Fig. 4). The two curves within the range $(\varepsilon_1^*, \varepsilon_2^*)$ in Fig. 3(a) turn into a vertical line. Since the boundary curves at point C are quite simple, a systematic procedure for designing δ and ε is expected to be simple. The procedure we propose is summarized by the following theorem.

Theorem 1 *Assume that the frequency of delay variation, Ω, is sufficiently large (i.e., $\omega \ll \Omega$) and oscillators (1) satisfy*

$$\mu < \omega(2 + \pi)/(4\pi). \tag{17}$$

If the amplitude of delay variation is set to $\delta = \pi/\omega$ and the coupling strength is chosen from the range

$$\varepsilon \in (\hat{\varepsilon} - \Delta\varepsilon, \hat{\varepsilon} + \Delta\varepsilon), \tag{18}$$

then the steady state $\boldsymbol{Z}^*$ of oscillators (1) coupled by connections (2) is stable for any long nominal delay time $\tau_0 > 0$, where

$$\hat{\varepsilon} := \left(\frac{2 + \pi}{2\pi}\right)\omega, \ \Delta\varepsilon := \frac{1}{2\pi}\sqrt{\omega(2 + \pi)\left\{\omega(2 + \pi) - 4\pi\mu\right\}}.$$

PROOF. The proof is given in two parts.

(I) For $\varepsilon = \hat{\varepsilon}$ and $\tau_0 \to +\infty$, all of the roots λ of the equations $g_{1,2}(\lambda) = 0$ lie in the open left-half complex plane.

(II) For all $\varepsilon \in (\hat{\varepsilon} - \Delta\varepsilon, \hat{\varepsilon} + \Delta\varepsilon)$, none of the roots λ for the equations $g_{1,2}(\lambda) = 0$ crosses the imaginary axis for any $\tau_0 > 0$.

The above two statements guarantee that $g_{1,2}(\lambda) = 0$ have no root in the open right-half complex plane for any $\varepsilon \in (\hat{\varepsilon} - \Delta\varepsilon, \hat{\varepsilon} + \Delta\varepsilon)$ and for any $\tau_0 > 0$. These statements are proven separately in the following.

(I) For $\tau_0 \to +\infty$, we have

$$\lim_{\tau_0 \to +\infty} g_{1,2}(\lambda) = (\lambda - \mu + \varepsilon + i\omega)(\lambda - \mu + \varepsilon - i\omega).$$

Substituting $\varepsilon = \hat{\varepsilon}$ into the above equation, the real part of the roots is given by $\mathrm{Re}(\lambda) = \mu - \omega(2+\pi)/(2\pi)$. From assumption (17), the inequality $\mathrm{Re}(\lambda) < 0$ holds.

(II) Statement (II) is equivalent to stating that there is no real root λ_I for $F(\varepsilon, \lambda_I) = 0$ with $\forall \varepsilon \in (\hat{\varepsilon} - \Delta\varepsilon, \hat{\varepsilon} + \Delta\varepsilon)$. Therefore, the condition

$$F(\varepsilon, \lambda_I) > 0, \ \forall \varepsilon \in (\hat{\varepsilon} - \Delta\varepsilon, \hat{\varepsilon} + \Delta\varepsilon), \ \forall \lambda_I \in \mathbb{R}, \tag{19}$$

is a sufficient condition for statement (II). Let us introduce a new function:

$$\underline{F}(\varepsilon, \lambda_I) := (\varepsilon - \mu)^2 + (\lambda_I - \omega)^2 - \varepsilon^2 \Gamma\left(\frac{\pi}{\omega}\lambda_I\right),$$

where Γ is denoted by

$$\Gamma(x) := \begin{cases} -2(x - \pi)/(2 + \pi) & x \leq \pi, \\ +2(x - \pi)/(2 + \pi) & x \geq \pi. \end{cases}$$

Appendix A guarantees that $F(\varepsilon, \lambda_I) \geq \underline{F}(\varepsilon, \lambda_I)$ holds for all $\lambda_I \in \mathbb{R}$. Instead of condition (19), we shall prove

$$\underline{F}(\varepsilon, \lambda_I) > 0, \ \forall \varepsilon \in (\hat{\varepsilon} - \Delta\varepsilon, \hat{\varepsilon} + \Delta\varepsilon), \ \forall \lambda_I \in \mathbb{R}. \tag{20}$$

Note that $\underline{F}(\varepsilon, \lambda_I) > 0$ holds if the following two conditions are satisfied: i) $\underline{F}(\varepsilon, \lambda_I) = 0$ with $\forall \varepsilon \in (\hat{\varepsilon} - \Delta\varepsilon, \hat{\varepsilon} + \Delta\varepsilon)$ has no real roots λ_I; ii) there exists λ_I such that $\underline{F}(\varepsilon, \lambda_I) > 0$ with $\forall \varepsilon \in (\hat{\varepsilon} - \Delta\varepsilon, \hat{\varepsilon} + \Delta\varepsilon)$. We first consider condition i). Since $\underline{F}(\varepsilon, \lambda_I)$ is symmetric to $\lambda_I = \omega$, it is sufficient to consider only $\lambda_I \leq \omega$. The equation $\underline{F}(\varepsilon, \lambda_I) = 0$ for $\lambda_I \leq \omega$ is given by

$$\lambda_I^2 + 2\lambda_I \left\{ \frac{\pi\varepsilon^2}{(2 + \pi)\omega} - \omega \right\} + \omega^2 + (\varepsilon - \mu)^2 - \frac{2\pi\varepsilon^2}{2 + \pi} = 0.$$

If the following inequality is satisfied:

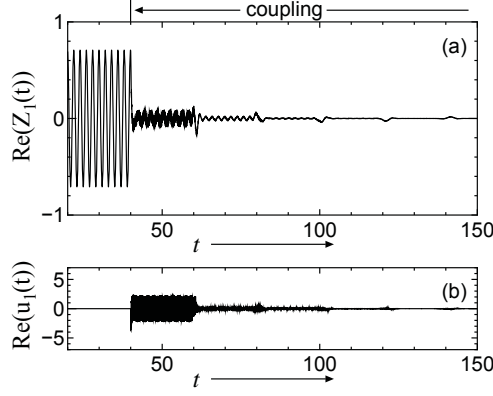$$\pi\varepsilon^2 - (2 + \pi)\omega\varepsilon + \mu(2 + \pi)\omega < 0, \tag{21}$$

9

Fig. 5. Time series data of oscillators (1) coupled by connections (2). The parameters are set to $\omega = \pi$, $\mu = 0.5$, $\delta = 1$, $\varepsilon = 3.0$, $\tau_0 = 20$, and $\Omega = 10\pi$. The oscillators are coupled at $t = 40$. (a) Real part of $Z_1(t)$. (b) Real part of $u_1(t)$.

then $\underline{F}(\varepsilon, \lambda_I) = 0$ has no real roots. Inequality (21) holds for all $\varepsilon \in (\hat{\varepsilon} - \Delta\varepsilon, \hat{\varepsilon} + \Delta\varepsilon)$. For condition ii), we easily obtain

$$\underline{F}(\varepsilon, \omega) = (\varepsilon - \mu)^2 > 0, \ \forall \varepsilon \in (\hat{\varepsilon} - \Delta\varepsilon, \hat{\varepsilon} + \Delta\varepsilon).$$

Statement (II) has thus been proven by conditions i) and ii). □

5 Discussions and summary

We design the coupling parameters δ and ε for given $\mu = 0.5$ and $\omega = \pi$ in accordance with Theorem 1. The frequency Ω is set to a large value $\Omega = 10\pi$. Assumption (17), i.e., $0.5 < 1.285$, is confirmed to hold. The amplitude is fixed at $\delta = \pi/\omega = 1$. Range (18) is estimated as $\varepsilon \in (0.562, 4.580)$. Then, the coupling strength is set to $\varepsilon = 3.0$. The behavior of the oscillators coupled by a long-delay connection $\tau_0 = 20$ is shown in Fig. 5. The state variable $\mathrm{Re}(Z_1(t))$ and the coupling signal $\mathrm{Re}(u_1(t))$ converge to zero after coupling. This is the amplitude death induced by the time-varying long-delay connection.

It is well known that the delayed feedback control [28,29] never stabilizes the unstable fixed points which satisfy the *odd number property* [30,31]. Konishi reported that this property remains in oscillators coupled by time delay connections [5]. According the stability analysis on the previous work [5], it is easy to confirm that the property still remains in oscillators coupled by time-varying delay connections.

Although, to the authors' knowledge, there have been few efforts to investigate a pair of oscillators coupled by time-varying delay connections, some previous studies are related to our results, and these studies are reviewed below.

10

Gjurchinovski and Urumov investigated the stabilization of unstable fixed points in single oscillators by a time-varying delay feedback control [26]. They applied an important result reported in Ref. [25] to chaotic oscillators. The results of the present study can be considered as an extension of their study [26] to amplitude death in a pair of coupled oscillators.

Atay reported that distributed delay connections facilitate amplitude death [14]. The dynamics of oscillators coupled by the distributed delay connections is quite similar to that coupled by time-varying delay connections when Ω is sufficiently large. Compared with the Atay study, the present paper has the following two additional features. First, although realizing the distributed delay connection for practical systems would not be easy, the time-varying delay connection can be easily realized in experimental systems, such as laser systems. Second, we explicitly introduce a systematic procedure by which to design ε and δ for an arbitrary-long delay induced stabilization. Therefore, the present paper not only presents an analysis of the coupled oscillators, but also provides an easily implementable connection for facilitating amplitude death, which can be designed systematically.

In summary, we found connection parameters at which amplitude death can be induced by arbitrary-long delay connections. Furthermore, a simple systematic procedure by which to design such connection parameters was presented, and this procedure was verified by numerical simulation.

A   Proof of $F(\varepsilon, \lambda_I) \geq \underline{F}(\varepsilon, \lambda_I)$ for all $\lambda_I \in \mathbb{R}$

It is necessary to prove that $\mathrm{sinc}^2(x) \leq \Gamma(x)$ for all $x \in \mathbb{R}$, where the function $\mathrm{sinc}(x)$ is defined by

$$\mathrm{sinc}(x) := \begin{cases} (\sin x)/x & \text{if } x \neq 0, \\ 1 & \text{if } x = 0. \end{cases}$$

According to Reference [32], we have $\mathrm{sinc}(x) = \cos(x/2)\mathrm{sinc}(x/2)$. Since $\mathrm{sinc}^2(x/2) \leq 1$ holds, we obtain

$$\mathrm{sinc}^2(x) \leq \cos^2(x/2) = (\cos x + 1)/2. \tag{A.1}$$

We notice

$$\cos x \leq \Lambda(x) \leq 2\Gamma(x) - 1, \tag{A.2}$$

11

where $\Lambda(x)$ is defined by

$$\Lambda(x) := \begin{cases} -x + \pi/2 & \text{if } \pi/2 - 1 \leq x \leq \pi/2, \\ -2x/\pi + 1 & \text{if } \pi/2 \leq x \leq \pi, \\ +2x/\pi - 3 & \text{if } \pi \leq x \leq 3\pi/2, \\ x - 3\pi/2 & \text{if } 3\pi/2 \leq x \leq 3\pi/2 + 1, \\ 1 & \text{if } x \leq \pi/2 - 1 \ \text{ or } \ 3\pi/2 + 1 \leq x. \end{cases}$$

From inequalities (A.2) and (A.1), the simple relation $\text{sinc}^2(x) \leq \Gamma(x)$ allows us to prove the following inequality:

$$F(\varepsilon, \lambda_I) \geq (\varepsilon - \mu)^2 + (\lambda_I - \omega)^2 - \varepsilon^2 \Gamma\left(\lambda_I \pi/\omega\right) =: \underline{F}(\varepsilon, \lambda_I),$$

for all $\lambda_I \in \mathbb{R}$.

References

[1] A. Pikovsky, M. Rosenblum, J. Kurths, Synchronization, Cambridge University Press, 2001.

[2] P. Holmes, R. Full, D. Koditschek, J. Guckenheimer, SIAM Review 48 (2006) 207–304.

[3] Y. Yamaguchi, H. Shimizu, Physica D 11 (1984) 212–226.

[4] D. Aronson, G. Ermentout, N. Kopell, Physica D 41 (1990) 403–449.

[5] K. Konishi, Phys. Lett. A 341 (2005) 401–409.

[6] D. Reddy, A. Sen, G. Johnston, Phys. Rev. Lett. 80 (1998) 5109–5112.

[7] S. Strogatz, Nature 394 (1998) 316–317.

[8] D. Reddy, A. Sen, G. Johnston, Phys. Rev. Lett. 85 (2000) 3381–3384.

[9] R. Herrero, M. Figueras, J. Rius, F. Pi, G. Orriols, Phys. Rev. Lett. 84 (2000) 5312–5315.

[10] D. Reddy, A. Sen, G. Johnston, Physica D 129 (1999) 15–34.

[11] K. Konishi, Phys. Rev. E 67 (2003) 017201.

[12] K. Konishi, Phys. Rev. E 70 (2004) 066201.

[13] M. Mehta, A. Sen, Phys. Lett. A 355 (2006) 202–206.

[14] F.M. Atay, Phys. Rev. Lett. 91 (2003) 094101.

[15] F.M. Atay, Physica D 183 (2003) 1–18.

[16] F.M. Atay, Journal of Differential Equations 221 (2006) 190–209.

[17] A. Prasad, Phys. Rev. E 72 (2005) 056204.

[18] R. Karnatak, R. Ramaswamy, A. Prasad, Phys. Rev. E 76 (2007) 035201.

[19] R. Karnatak, R. Ramaswamy, A. Prasad, Chaos 19 (2009) 033143.

[20] K. Konishi, K. Senda, H. Kokame, Phys. Rev. E 78 (2008) 056216.

[21] J. Yang, Phys. Rev. E 76 (2007) 016204.

[22] R. Vicente, S. Tang, J. Mulet, C. R. Mirasso, J.-M. Liu, Phys. Rev. E 73 (2006) 047201.

[23] K. Konishi, H. Kokame, Proc. of International Symposium on Nonlinear Theory and its Applications (2008) 528–531.

[24] K. Konishi, H. Kokame, N. Hara, Proc. of Second IFAC meeting related to analysis and control of chaotic systems (2009).

[25] W. Michiels, V. V. Assche, S.-I. Niculescu, IEEE Trans. Automatic Control 50 (2005) 493– 504.

[26] A. Gjurchinovski, V. Urumov, Europhysics Letters 84 (2008) 40013.

[27] Y. Kuramoto, Chemical Oscillations, Waves and Turbulance, Springer-Verlag, 1984.

[28] K. Pyragas, Phys. Lett. A 170 (1992) 421–428.

[29] K. Pyragas, Philosophical Transactions of the Royal Society A 364 (2006) 2309–2334.

[30] T. Ushio, IEEE Trans. Circuits and Sys. I 43 (1996) 815–816.

[31] H. Kokame, K. Hirata, K. Konishi, T. Mori, IEEE Trans. on Automatic Control 46 (2001) 1908–1913.

[32] W. Gearhart, H. Shultz, College Mathematics Journal 21 (1990) 90–99.